Supplementary Information

1. Synthesis

According to previous reports, carbon spheres (CS) were synthesized by hydrothermal method using glucose as raw material. The 0.5 mol glucose was dissolved in 40 mL deionized water, stirred for 15 min and placed in a 50 mL autoclave (lined with polytetrafluoroethylene). Subsequently, it was naturally cooled to room temperature after 7 h at 170-180 °C. After ultrasonic washing and centrifugation, the samples were dried at 80 °C for 8 h in a vacuum dryer to obtain CS material.

TDA@LDH/CS materials were prepared by co-precipitation method under supersaturated conditions. $MgCl_2 \cdot 6H_2O$ and $AlCl_3 \cdot 6H_2O$ were dissolved in 40 mL deionized water with Mg^{2+} / Al^{3+} molar ratio of 5 : 1. Then 0.3 g CS and 3 mL TDA were added into the salt solution, ultrasonic stirring 30min as the precursor solution. Then, the precursor salt solution was added dropwise to 100 mL NaOH solution (2 $mol \cdot L^{-1}$), and the final pH value was controlled at 13 ± 0.1. It was then stirred at room temperature for 4 hours, and then placed in a 60 °C water bath for 12 hours of aging. The aged liquid was then washed by centrifugation at 8000 $r \cdot min^{-1}$ until the supernatant was neutral. Finally, the precipitated solid was dried at 80 °C to prepare TDA@LDH/CS. Similarly, LDH/CS materials and LDH materials were prepared under the same conditions.

2. Characterization

The phase constituents and crystal structure were determined using XRD (Rigaku Ultima IV, Japan) with Cu Kαradiation at 2θ from 5° to 90°. The surface functional groups of the composites were tested by FTIR (Bruker Alpha, Germany), and the spectra of 400-4000 cm^{-1} were recorded. The surface morphology and elemental composition of the samples was performed using SEM (ZEISS Sigma 300,Germany) and EDS (Oxford，Britain). The porosity and surface area were calculated using a BET

analyzer under atmospheric nitrogen conditions (ASAP 2460,USA), while the pore size distribution

(PSD) was estimated by the Barrett−Joyner−Halenda (BJH) theory. The surface elements of the

composites before and after modification were measured by an XPS measurement (Thermo Scientific

K-Alpha, USA). TG curves for the sorbents were determined by using a Mettler TGA/DSC

thermogravimetric analyzer (TG 209 F3 Nevio, Germany) at a heating rate of 10 ℃/min from 30 ℃ to

700 ℃ under N_2 flow. Indirect determination of zero point charge (pH_{pzc}) of composites by "drift

method".

3. Calculation Method

（1）The adsorption capacities at interval time Q_t (mg·g^{-1}) and equilibrium time Qe (mg·g^{-1}) ,

respectively, are calculated as below：

$$Q_t = \frac{(C_0 - C_t) \ V}{m}$$
（S-1）

$$Q_t = \frac{(C_0 - C_e) \ V}{m}$$
（S-2）

Where C_0 (mg·L^{-1}), C_t (mg·L^{-1}), and C_e (mg·L^{-1}) are the concentrations of nitrite at the initial

time, interval time, and equilibrium time, respectively; m (g) is the weight of the as-synthesized

samples; V (L) is the volume of the aqueous solution.

The calculation expressions related to removal rate (RE) is as follows:

$$RE = \frac{C_0 - C_t}{C_0}$$
（S-3）

（2）The models used for adsorption kinetics is as follows：

Pseudo-first-order model:

$$Q_t = Q_e \ (1 - e^{-k_1 t})$$
（S-4）

Pseudo-second-order model:

$$Q_t = \frac{k_2 Q_e^2 t}{1 + k_2 Q_e t}$$

（S-5）

Intraparticle diffusion model:

$$Q_t = k_i t^{\frac{1}{2}} + C$$

（S-6）

Where k_1 (min^{-1}), k_2 (g·mg^{-1}·min^{-1}), k_i (mg·g^{-1}·min$^{-1/2}$) are the rate constant for the corresponding

model in the Exp (4-6), C (mg·g^{-1}) is the intercept.

（3）The adsorption thermodynamics and adsorption isotherm models are as follows：

Langmuir model:

$$Q_e = \frac{Q_m K_L C_e}{1 + K_L C_e}$$

（S-7）

Freundlich model:

$$Q_e = K_F C_e^n$$

（S-8）

Temkin model:

$$Q_e = b_T ln（K_T C_e）$$

（S-9）

Redlich-Peterson (R-P)model：

$$Q_e = \frac{K_R C_e}{1 + K_p C_e^g}$$

（S-10）

Where C_e (mg·L^{-1})is the equilibrium concentration; Q_m(mg·g^{-1}) is the maximum adsorption

capacity , K_L(L·mg^{-1}) is the adsorption equilibrium constant of Langmuir adsorption isotherm mode;

K_F(mg·g^{-1}) is the empirical constant of Freundlich model (mg·g^{-1}); K_T (L·mg^{-1}) is the equilibrium

binding constant (L·mg^{-1}), b_T (J·mol^{-1}) is the Temkin constant.

Van't Hoff equation:

$$\Delta G^0 = - RT ln K_c$$

（S-11）

$$K_c = 55.5 \times 1000 \times K_L M_A \qquad \text{(S-12)}$$

$$lnK_c = -\frac{\Delta H^0}{RT} + \frac{\Delta S^0}{R} \qquad \text{(S-13)}$$

where R is the ideal gas constant (8.314 J/mol·K), K_C is denoted thermodynamic equilibrium constant (dimensionless). The factor 55.5 is the number of moles of pure water per liter (1000 g/L divided by 18g/mol), and K_L (L/mg) is the Langmuir adsorption equilibrium constant, M_A is the molecular weight of the adsorbate (NO_3^--N)) (g/mol).

4. Characterization and experimental results

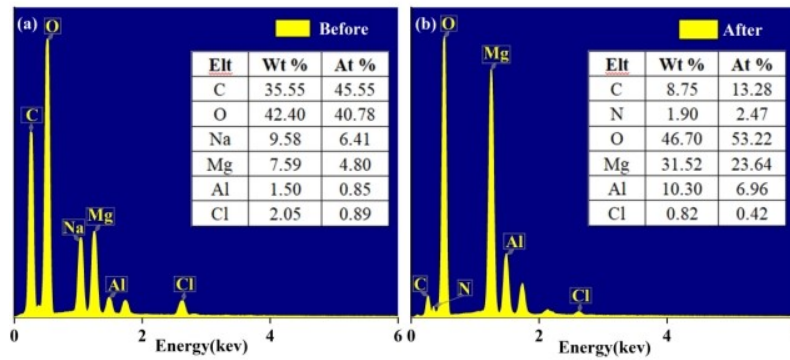(1) The EDS spectra of the composites before and after adsorption are shown in **Fig. S1.**

Fig. S1. EDS patterns of TDA@LDH/CS (a) before and (b) after adsorption.
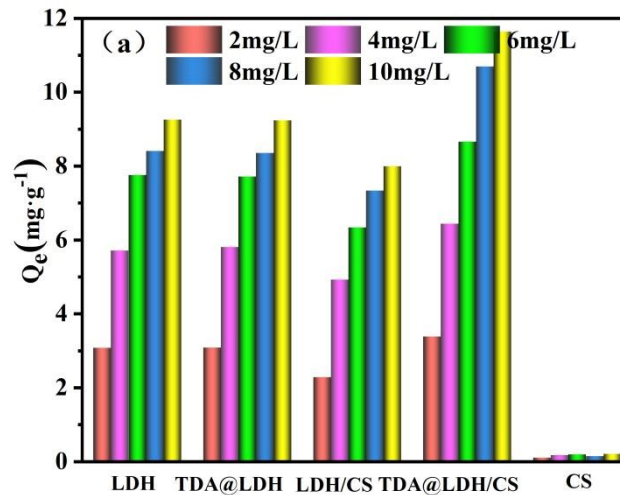

Fig.S2 Comparison of the adsorption capacities of LDH, LDH/CS, CS and TDA@LDH/CS on NO_3^- at various concentrations, T =298 K, dosage(m/V) =0.5 g/L.

(2) **Table S1.** The BET specific surface area and pore size distribution of LDH, LDH/CS and TDA@LDH/CS

	S_{BET} $(m^2 \cdot g^{-1})$	V_p $(cm^3 \cdot g^{-1})$	D_{BJH} (nm)
LDH	32.25	0.24	17.52
LDH/CS	46.41	0.12	5.72
TDA@LDH/CS	67.15	0.26	10.57

S_{BET}: area by BET method; V_p: total pore volume; D_{BJH}: pore diameter in desorption.

(3) The zero point charge (pH_{pzc}) of the composite was determined regarding the pH drift method. 0.1 g TDA@LDH/CS composite and 50 mL NaCl solution were mixed in 100 mL conical flask and adjusted the initial pH values ($pH_{Initial}$) of NaCl solution from 2 to 12 with HCl and NaOH, the final pH values (pH_{Final}) was measured after occasional shaking for 24 h . The pH_{PZC} of the composite was discovered at $\Delta pH = 0$ ($\Delta pH = pH_{Final} - pH_{Initial}$).
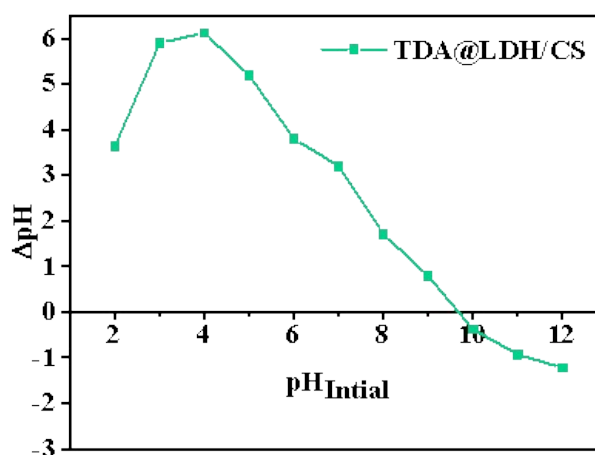

Fig. S3. Point of zero charge of TDA@LDH/CS

Table S2 The analysis of the dissolved ions in solution after adsorption of NO_3^- at pH=7±0.1.

Test batch	Ions concentration (mg/L) Mg^{2+}	Al^{3+}
1	0.115	0.022
2	0.168	0.069
3	0.066	0.042

(4) The relevant parameters of the intraparticle diffusion model are shown in **Table S3**.

Table S3. Comparison of the removal rate constants with other adsorbents

Adsorbents	Rate Constant (g/mg·min)	References
MgAl-modified biochar	0.005	[1]
ZnAl-LDH	0.04	[2]
ZnFe-LDHs-activated carbon	0.008	[3]
ZnAl-LDHs/activated carbon composite	0.01	[4]
MgFe-LDH/biochar	0.10	[5]
TDA@LDH/CS	0.11	This study

Table S4. Intraparticle diffusion data of TDA@LDH/CS for the removal of NO_3^-

C_0 (mg·L^{-1})	First stage		Second stage	
	k_1	R^2	k_2	R^2
2	0.31	1.00	0.05	0.95
4	0.78	0.94	0.07	1.00
6	0.89	0.92	0.07	0.98
8	1.10	0.93	0.05	0.99
10	0.96	0.92	0.16	0.99

(5) The XRD calculation results of crystal lattice parameters were shown in **Table S5**

Table S5. XRD data of TDA@LDH/CS before and after adsorption.

Sample	$D_{(003)}$(Å)	$D_{(110)}$(Å)	a(Å)	c(Å)	Interlayer distance (Å)
Before adsorption	8.11	1.54	3.08	24.33	**3.31**
After adsorption	8.01	1.54	3.08	24.03	**3.21**

* a= 2d$_{(110)}$;   c= 3d$_{(003)}$; Interlayer distance=d$_{(003)}$ - 4.8Å

References：

[1] Yin Q, Wang R, Zhao Z. Application of Mg–Al-modified biochar for simultaneous removal of

ammonium, nitrate, and phosphate from eutrophic water[J]. Journal of Cleaner Production, 2018, 176: 230-240.

[2] Islam M, Patel R. Synthesis and physicochemical characterization of Zn/Al chloride layered double hydroxide and evaluation of its nitrate removal efficiency[J]. Desalination, 2010, 256(1-3): 120-128.

[3] Karthikeyan P, Meenakshi S. Enhanced removal of phosphate and nitrate ions by a novel ZnFe LDHs-activated carbon composite[J]. Sustainable Materials and Technologies, 2020, 25: e00154.

[4] Karthikeyan P, Meenakshi S. Synthesis and characterization of Zn–Al LDHs/activated carbon composite and its adsorption properties for phosphate and nitrate ions in aqueous medium[J]. Journal of Molecular Liquids, 2019, 296: 111766.

[5] Xue L, Gao B, Wan Y, et al. High efficiency and selectivity of MgFe-LDH modified wheat-straw biochar in the removal of nitrate from aqueous solutions[J]. Journal of the Taiwan Institute of Chemical Engineers, 2016, 63: 312-317.